Geophys. J. Int. (1994) **119,** 857–868

Asymptotic theory for diffusive electromagnetic imaging

Jean Virieux,[1] Carlos Flores-Luna[1,2] and Dominique Gibert[3]

[1] *Institut de Géodynamique, UNSA Rue Albert Einstein,* 06560 *Valbonne, France*
[2] *CICESE, Depto. Geofisica Aplicada KM* 107 *Carretera. Tijuana-Ensenada, Ensenada* 22800, *Baja California, Mexico*
[3] *Geosciences Rennes, Rennes* I *Avenue Général Leclerc,* 35042 *Rennes cédex, France*

Accepted 1994 June 6. Received 1994 June 6; in original form 1993 August 4

SUMMARY

We propose an asymptotic theory for diffusive electromagnetic imaging. Three steps

E can be written $(0, E_y, 0)$ and we assume invariance in the y-direction. The magnetic susceptibility field **H** has only two

wave $\exp(\mathbf{k} \cdot \mathbf{x})$ with $-i\omega\sigma_0\mu_0 = k^2$. The selection of the square root of $-i$ is such that the plane-wave amplitude

solution and our numerical attempt to estimate the accuracy of 2-D geometrical reconstructions.

ASYMPTOTIC SOLUTION FOR A SMOOTH MEDIUM

Let us assume now that the medium has a smooth variation of the conductivity $\sigma(\mathbf{x})$. We look for a solution in the frequency domain which behaves as

$$e^{-\sqrt{-i\omega}\,\tau(\mathbf{x})} \sum_{k=0}^{+\infty} \frac{A_k(\mathbf{x})}{(\sqrt{-i\omega})^k}. \tag{9}$$

This ansatz for the solution is the one used in the ray theory except that the $i\omega$ term for wave propagation has been replaced by $-\sqrt{-i\omega}$ for diffusive transport. It has been previously proposed by Tikhonov (1965) on a purely theoretical basis. This term has no obvious property in the Fourier domain as the translation property of the exponential terms. Nevertheless, we have already constructed an analytical solution in the previous section with this factor. The function τ will be called the pseudo-phase function following previous works on the link between

the origin, the diffusive and propagation solutions are, respectively,

$$\begin{aligned} e^{-\sqrt{-i\omega}\,\tau(\mathbf{x})} A_0(\mathbf{x}) &\to A_0(\mathbf{x}) \frac{\tau(\mathbf{x})}{2\sqrt{\pi t^3}} e^{-\tau^2(\mathbf{x})/4t} H(t), \\ e^{i\omega T(\mathbf{x})} A_0(\mathbf{x}) &\to A_0(\mathbf{x}) \delta[t - T(\mathbf{x})], \end{aligned} \tag{11}$$

in a 3-D medium. These solutions have a very simple geometrical interpretation. The wave solution is the delta source signal shifted by the traveltime T and scaled by A_0 (Fig. 1). The diffusive solution is more complex to analyse: the delta source signal is transformed into a localized damped function maximum at $\tau^2/6$ (Fig. 2) which is similar to a phase shift although the diffusive energy stays around the source. The geometrical effect of the 2-D medium will add a tail to both signals, while reducing down to the 1-D geometry again deforms the signal. The geometry of medium influences the propagation and diffusion of the signal as summarized in Fig. 1 and Fig. 2. The diffusion solution (11) adds an extra difficulty because it exhibits a time decrease of $1/\sqrt{t^3}$ which is converted in a $1/t$ decrease in the 2-D case and $1/\sqrt{t}$ in the 1-D case. In our numerical illustrations, we shall only use the 2-D geometry for both sources and medium.

The smearing of the diffusive solution is the feature

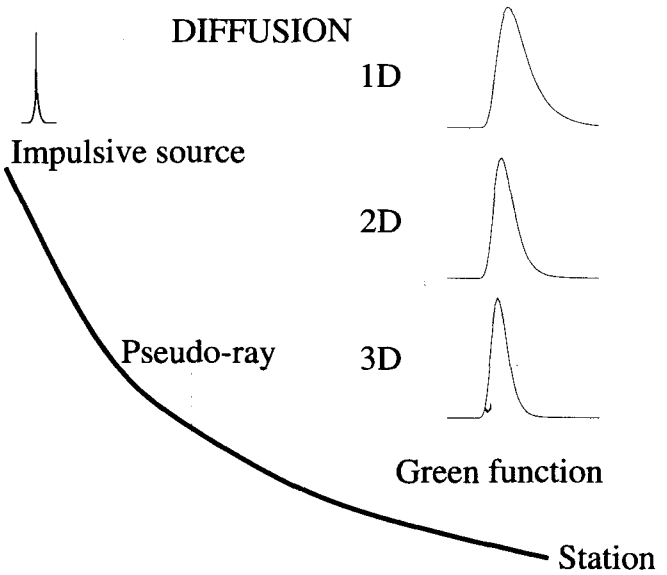

Figure 2. Diffusion of the impulsive signal from a source along a pseudo-ray. Note the less dramatic difference of shape compared with wave propagation arising from the medium geometry.

The transport equation which is the second one we are interested in gives the evolution of the amplitude term as we move along the ray. One finds an estimation of the amplitude at s' from s

$$A_0(s') = A_0(s)\frac{\sqrt{u[\mathbf{x}(s)]J(s)}}{\sqrt{u[\mathbf{x}(s')]J(s')}}, \tag{12}$$

where J is the Jacobian used in the definition of an elementary surface perpendicular to the ray parameterized by two coordinates γ_1 and γ_2 associated with the curvilinear coordinate s.

The electrical field will be in the frequency domain

$$\frac{1}{\sqrt{u(z)J(z)}}\mathrm{e}^{-\sqrt{-i\omega}\,\tau(z)}S(\omega)\phi(\gamma_1, \gamma_2), \tag{13}$$

where $S(\omega)$ is the Fourier transform of the time function of the source and ϕ is the intensity of the electromagnetic source. The pseudo-phase τ is equal to $r\sqrt{\mu_0\sigma(r)} = ru(r)$.

In order to estimate the intensity ϕ of eq. (13), we might look at a canonical problem where the high-frequency solution is known. Fortunately, a solution given by eq. (8) exists for a homogeneous medium which has been constructed in the previous section. Because the Jacobian is equal to r in a 2-D homogeneous medium, we deduce the intensity for an isotropic source at the origin

$$\phi(\gamma_1, \gamma_2) = \sqrt{2\pi} \tag{14}$$

valid for a smoothly varying medium by identification with the solution (8). The asymptotic solution in a 2-D smooth varying medium for a $\mathbf{r}_s$ source is

$$E_y^0(\mathbf{r}, \mathbf{r}_s, \omega) = A_0(\mathbf{r}, \mathbf{r}_s)\mathrm{e}^{-\sqrt{-i\omega}\,\tau(\mathbf{r},\mathbf{r}_s)}\frac{1}{\sqrt{\sqrt{-i\omega}}}\sqrt{2\pi} \tag{15}$$

where we have again introduced the specific frequency-dependent factor for the 2-D geometry already mentioned in the previous paragraph.

Let us underline again that this solution is only approximate in a 2-D homogeneous medium while the corresponding solution for 1-D and 3-D homogeneous media are exact solutions. Considering asymptotic solutions is a valid assumption, especially when the background medium is nearly homogeneous.

BORN APPROXIMATION

Let us now consider a perturbation of the conductivity. Because in this paper we assume an invariance along the direction y, we consider a 2-D reference medium with a smoothly varying conductivity $\sigma_0(\mathbf{x})$. For a point source (a line source in a 3-D medium with one invariant direction) at the source position $\mathbf{r}_s$, the Green function at position $\mathbf{r}$ is denoted $E_y^0(\mathbf{r}, \mathbf{r}_s)$. We want to study media slightly different from this smooth reference medium by a conductivity perturbation given by $\sigma(\mathbf{x}) = \sigma_0(\mathbf{x}) + \Delta\sigma(\mathbf{x})$. We assume that the magnetic permeability μ_0 remains constant. The Green function E_y will be split into the known Green function E_y^0 and the perturbation ΔE_y. The equation

$$\sigma(\mathbf{x})i\omega\mu_0 E_y(\mathbf{r}, \mathbf{r}_s) + \nabla^2 E_y(\mathbf{r}, \mathbf{r}_s) = -4\pi\delta(\mathbf{r} - \mathbf{r}_s) \tag{16}$$

is expanded into

$$\sigma_0(\mathbf{x})i\omega\mu_0\,\Delta E_y + \nabla^2\,\Delta E_y = -4\pi[i\omega\mu_0\Delta\sigma(\mathbf{x})E_y/4\pi], \tag{17}$$

the solution of which can be written as a convolution of the Green function E_y^0, solution of the left-hand side of eq. (17), and the source term $i\omega\mu_0\,\Delta\sigma(\mathbf{x})E_y/4\pi$ leading to

$$\Delta E_y(\mathbf{r}, \mathbf{r}_s, \omega) = \frac{i\omega\mu_0}{4\pi}\int_{\mathcal{M}} E_y(\mathbf{r}, \mathbf{x}, \omega)\,\Delta\sigma(\mathbf{x})E_y^0(\mathbf{x}, \mathbf{r}_s, \omega)\,d\mathbf{x}^2, \tag{18}$$

where the domain of integration $\mathcal{M}$ is over diffracting points $\mathbf{x}$. The first-order Born approximation is obtained by replacing E_y with E_y^0 in the integral, leading to a linear functional between $\Delta\sigma$ and ΔE_y:

$$\Delta E_y(\mathbf{r}, \mathbf{r}_s, \omega) = \frac{i\omega\mu_0}{4\pi}\int_{\mathcal{M}} E_y^0(\mathbf{r}, \mathbf{x}, \omega)\,\Delta\sigma(\mathbf{x})E_y^0(\mathbf{x}, \mathbf{r}_s, \omega)\,d\mathbf{x}^2. \tag{19}$$

Assuming now that solutions have the asymptotic form in the smooth reference 2-D medium

$$E_y^0(\mathbf{x}, \mathbf{r}_s, \omega) = A_0(\mathbf{x}, \mathbf{r}_s)\mathrm{e}^{-\sqrt{-i\omega}\,\tau(\mathbf{x},\mathbf{r}_s)}\frac{1}{\sqrt{\sqrt{-i\omega}}}\sqrt{2\pi}$$

$$E_y^0(\mathbf{r}, \mathbf{x}, \omega) = E_y^0(\mathbf{x}, \mathbf{r}, \omega) \tag{20}$$

$$= A_0(\mathbf{r}, \mathbf{x})\mathrm{e}^{-\sqrt{-i\omega}\,\tau(\mathbf{r},\mathbf{x})}\frac{1}{\sqrt{\sqrt{-i\omega}}}\sqrt{2\pi},$$

we obtain for a given couple of (source, receiver) the simple relation

$$\Delta E_y(\mathbf{r}, \mathbf{r}_s, \omega) = \frac{i\omega\mu_0}{2}\int_{\mathcal{M}} \Delta\sigma(\mathbf{x})\,A_0(\mathbf{r}, \mathbf{x}, \mathbf{r}_s)\frac{\mathrm{e}^{-\sqrt{-i\omega}\,\tau(\mathbf{r},\mathbf{x},\mathbf{r}_s)}}{\sqrt{-i\omega}}d\mathbf{x}^2, \tag{21}$$

where

$$A_0(\mathbf{r}, \mathbf{x}, \mathbf{r}_s) = A_0(\mathbf{x}, \mathbf{r}_s)\, A_0(\mathbf{r}, \mathbf{x})$$
$$\tau(\mathbf{r}, \mathbf{x}, \mathbf{r}_s) = \tau(\mathbf{x}, \mathbf{r}_s) + \tau(\mathbf{r}, \mathbf{x}), \tag{22}$$

come from the product of the Green function connecting the source and the diffracting point and the Green function connecting the diffracting point and the receiver.

The asymptotic form has simplified the propagation of the field because ray tracing is symmetrical: the asymptotic

Expressions (21) and (23) are valid in a 2-D or a 3-D medium with an invariance in the y-direction for the definition of the TE mode. Expressions (21) in the frequency domain and (23) in the time domain are our basic linearized forward modelling for which we shall construct an inverse operator. The technique has been previously proposed by Jin *et al.* (1992) based on the work performed by Beylkin (1985) and Beylkin & Burridge (1990) among others on asymptotic Radon transforms.

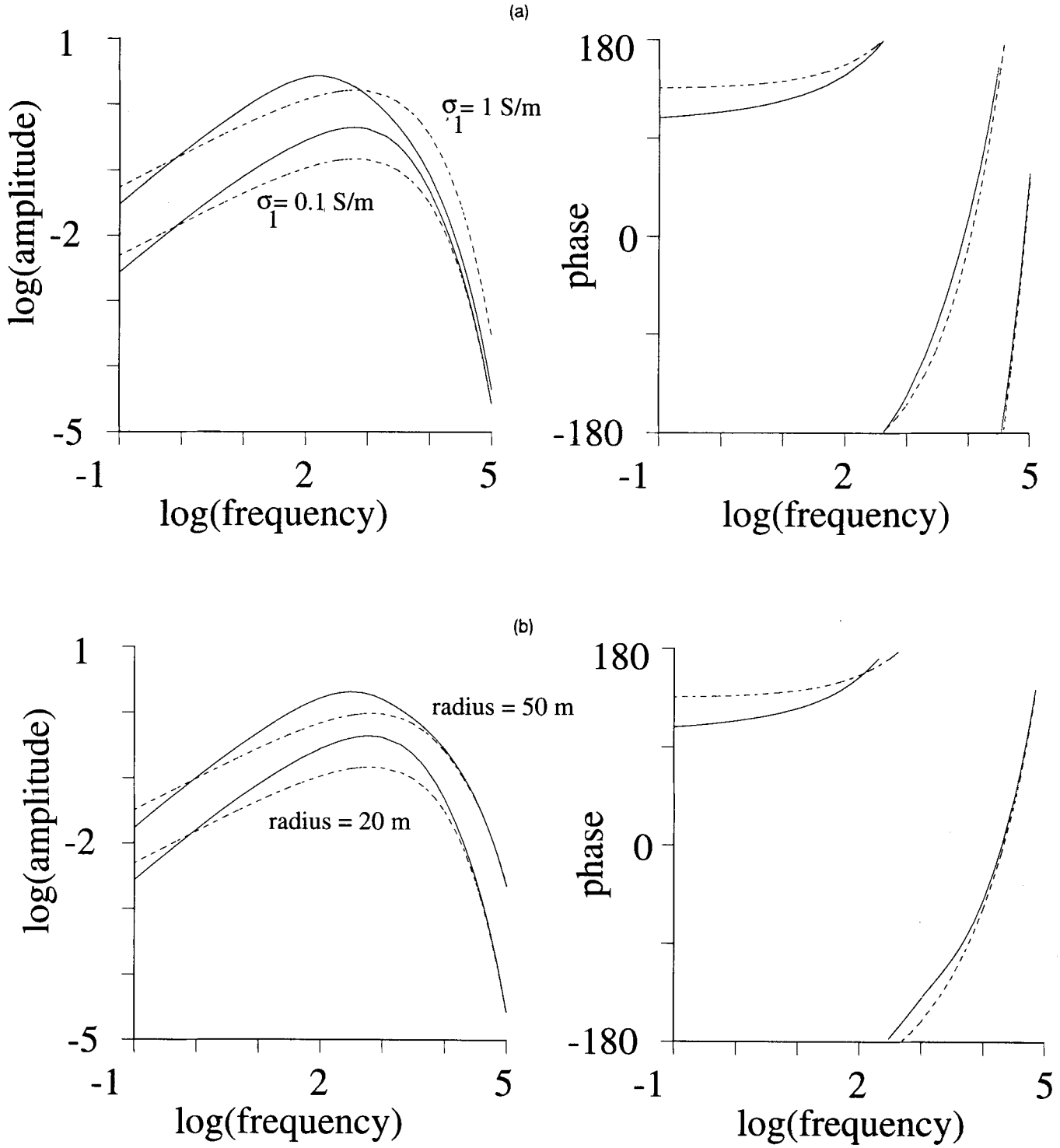

Figure 4. (a) Comparison between the exact solution and the Born approximation for a cylinder diffractor of radius 20 m. Notice the disagreement introduced by the Born approximation when the contrast of conductivity increases. For clarity, only the phase response for the

small perturbations of the conductivity and for small sizes of diffractor objects. We shall see in our inversion the effects of these disagreements. These effects will be the main limitation of our reconstruction technique.

We must remember that the main misfit arises from our transformation of the 2-D Green function into its high-frequency approximation. For 3-D and 1-D homogeneous media, the Green function agrees with its high-frequency approximation as we have checked. Therefore, we do expect better results with the Born approximation for 3-D structures.

ASYMPTOTIC INVERSION

In order to pose the inverse problem properly we must define both model and data spaces, and the operators between these two spaces. The model space $\mathcal{M}(\mathbf{x})$ is the space of all possible perturbations of the conductivity $\Delta\sigma$ at each point $\mathbf{x}$ of the medium. The data space consists of all electric perturbations of the TE mode for many sources $\mathbf{r}_s$ and receivers $\mathbf{r}$ at different frequencies. For simplicity of the analytical developments, we shall consider Fourier trans-

Inversion by a least-squares method

The definition of the misfit function requires an explicit definition of the inner product in data space:

$$\langle \Delta E_y \mid \Delta E'_y \rangle_{\mathscr{D}} = \sum_{\mathbf{r}_s,\mathbf{r}} \int_{\Omega} d\omega \, \Delta E_y^*(\mathbf{r}, \mathbf{r}_s, \omega) \times \mathbf{Q}(\mathbf{r}, \mathbf{x}_0, \mathbf{r}_s, \omega) \, \Delta E'_y(\mathbf{r}, \mathbf{r}_s, \omega) \tag{25}$$

where * denotes the complex conjugate. The sum and the integral extend over the data space $\mathscr{D}$. The covariance matrix $\mathbf{Q}$ is diagonal by construction with elements:

$$\mathbf{Q}(\mathbf{r}, \mathbf{x}_0, \mathbf{r}_s, \omega) = \frac{|\mathbf{p}(\mathbf{r}, \mathbf{x}_0, \mathbf{r}_s)|^2}{A^2(\mathbf{r}, \mathbf{x}_0, \mathbf{r}_s)} \frac{1}{\sqrt{-i\omega}} \tag{26}$$

where $\mathbf{p}(\mathbf{r}, \mathbf{x}_0, \mathbf{r}_s) = \nabla\tau(\mathbf{r}, \mathbf{x}_0, \mathbf{r}_s)$, is the gradient of the two-way pseudo-phase function τ (Fig. 5).

The particular form of the covariance matrix $\mathbf{Q}$ is introduced in order to correct for the decrease with distance and for the spectral content of the Green function. One can see in the definition of covariance matrix $\mathbf{Q}$ only the

integral operator $\mathbf{G}$, and defined by the classical relationship

$$\langle \Delta E_y \mid \mathbf{G}\,\Delta\sigma\rangle_{\mathcal{A}} = \langle \mathbf{G}^\dagger\,\Delta E_y \mid \Delta\sigma\rangle_{\mathcal{M}}, \tag{31}$$

while the generalized inverse G^{-g} is equal to $(\mathbf{G}^\dagger\mathbf{G})^{-1}\mathbf{G}^\dagger$.

Estimation of the gradient

The adjoint operator $\mathbf{G}^\dagger$ might be expressed by a kernel $\mathcal{K}$ with the following expression

$$\sum_{\mathbf{r}_s,\mathbf{r}} \int_\Omega d\omega \mathcal{K}(\mathbf{r},\mathbf{x},\mathbf{r}_s,\omega)\,\Delta E_y(\mathbf{r},\mathbf{r}_s,\omega), \tag{32}$$

where the reconstructed function is obtained at position $\mathbf{x}$ assuming a covariance $\mathbf{Q}$ depending on $\mathbf{x}_0$. From eq. (31) and from the forward problem (21),

$$\mathcal{K}(\mathbf{r},\mathbf{x},\mathbf{r}_s,\omega) = \frac{-1}{2}\mu_0 A(\mathbf{r},\mathbf{x},\mathbf{r}_s)\mathbf{Q}^*(\mathbf{r},\mathbf{x}_0,\mathbf{r}_s,\omega)\sqrt{-i\omega}^*\, e^{-\sqrt{-i\omega}^*\tau(\mathbf{r},\mathbf{x},\mathbf{r}_s)}. \tag{33}$$

The formal solution of the system (30) is

$$\Delta\sigma(\mathbf{x}_0) = H^{-1}(\mathbf{x}_0,\mathbf{x})\gamma^0(\mathbf{x}), \tag{34}$$

where

$$\gamma^0(\mathbf{x}) = \mathbf{G}^\dagger(\mathbf{r},\mathbf{x},\mathbf{r}_s)\,\Delta E_y^{\mathrm{obs}}(\mathbf{r},\mathbf{r}_s,\omega) \tag{35}$$

is the gradient of $S(\Delta\sigma)$ at $\Delta\sigma = 0$ and H is the Hessian giving the information of the curvature of the misfit function. Explicitly the gradient is given by

$$\gamma 0(\mathbf{x}) = \frac{-\mu_0}{2}\sum_{\mathbf{r}_s,\mathbf{r}}\int_\Omega d\omega \frac{A(\mathbf{r},\mathbf{x},\mathbf{r}_s)}{A^2(\mathbf{r},\mathbf{x}_0,\mathbf{r}_s)} \times |\mathbf{p}(\mathbf{r},\mathbf{x}_0,\mathbf{r}_s)|^2\, e^{-\sqrt{-i\omega}^*\tau(\mathbf{r},\mathbf{x},\mathbf{r}_s)}\,\Delta E_y^{\mathrm{obs}}(\mathbf{r},\mathbf{r}_s,\omega) \tag{36}$$

in the frequency domain. Expressing $\Delta E_y^{\mathrm{obs}}(\mathbf{r},\mathbf{r}_s,\omega)$ as the Fourier transform of $\Delta E_y^{\mathrm{obs}}(\mathbf{r},\mathbf{r}_s,t)$ leads to the following expression:

$$\gamma^0(\mathbf{x}) = -\frac{\mu_0}{2}\sum_{\mathbf{r}_s,\mathbf{r}}\int_T dt\,\Delta E_y^{\mathrm{obs}}(\mathbf{r},\mathbf{r}_s,t)\frac{A(\mathbf{r},\mathbf{x},\mathbf{r}_s)}{A^2(\mathbf{r},\mathbf{x}_0,\mathbf{r}_s)} \times |\mathbf{p}(\mathbf{r},\mathbf{x}_0,\mathbf{r}_s)|^2 \times \int_\Omega d\omega' e^{-\sqrt{-i\omega'}\tau(\mathbf{r},\mathbf{x},\mathbf{r}_s)} e^{-i\omega' t}. \tag{37}$$

We have used the complex conjugate operation giving $\sqrt{-i}^* = \sqrt{i}$ and the transformation of ω into $\omega' = -\omega$. By doing so, we are able to write the gradient as a single integral in the time domain

$$\gamma^0(\mathbf{x}) = -\frac{u_0\sqrt{\pi}}{2}\sum_{\mathbf{r}_s,\mathbf{r}}\frac{A(\mathbf{r},\mathbf{x},\mathbf{r}_s)}{A^2(\mathbf{r},\mathbf{x}_0,\mathbf{r}_s)}|\mathbf{p}(\mathbf{r},\mathbf{x}_0,\mathbf{r}_s)|^2 \times \int_T \mathrm{dt}\,\Delta E_y^{\mathrm{obs}}(\mathbf{r},\mathbf{r}_s,t)\frac{\tau(\mathbf{r},\mathbf{x},\mathbf{r}_s)}{t^{3/2}} e^{-\tau(\mathbf{r},\mathbf{x},\mathbf{r}_s)^2/4t} H(t). \tag{38}$$

Let us underline that the choice of the factor $\mathbf{Q}$ has modified the $t_{\max}$ compared with the one obtained for the forward linearized expression.

Asymptotic expression of the Hessian

The operator H^{-1} in eq. (34) is the formal inverse of $G^\dagger G$ and is very difficult to estimate for many inverse problems (see Jin *et al.* 1992, for a short discussion and Tarantola 1987, for an extensive review). In our approach, an asymptotic estimation is possible. We found from eqs (21) and (32) that

$$H(\mathbf{x},\mathbf{x}_0) = \frac{\mu_0^2}{4}\sum_{\mathbf{r}_s,\mathbf{r}}\frac{A(\mathbf{r},\mathbf{x},\mathbf{r}_s)}{A(\mathbf{r},\mathbf{x}_0,\mathbf{r}_s)}|\mathbf{p}(\mathbf{r},\mathbf{x}_0,\mathbf{r}_s)|^2 \times \int_\Omega d\omega\sqrt{-i\omega}\, e^{-\sqrt{-i\omega}^*\tau(\mathbf{r},\mathbf{x},\mathbf{r}_s)-\sqrt{-i\omega}\tau(\mathbf{r},\mathbf{x}_0,\mathbf{r}_s)}, \tag{39}$$

which reduces to

$$H(\mathbf{x},\mathbf{x}_0) = \frac{\mu_0^2}{4}\sum_{\mathbf{r}_s,\mathbf{r}}\frac{A(\mathbf{r},\mathbf{x},\mathbf{r}_s)}{A(\mathbf{r},\mathbf{x}_0,\mathbf{r}_s)}|\mathbf{p}(\mathbf{r},\mathbf{x}_0,\mathbf{r}_s)|^2 \times \int_0^\infty d\omega\sqrt{2\omega}\, e^{-\sqrt{\omega/2}[\tau(\mathbf{r},\mathbf{x}_0,\mathbf{r}_s)+\tau(\mathbf{r},\mathbf{x},\mathbf{r}_s)]} \times [\cos\{\sqrt{\omega/2}\,[\tau(\mathbf{r},\mathbf{x},\mathbf{r}_s)-\tau(\mathbf{r},\mathbf{x}_0,\mathbf{r}_s)]\} - \sin\{\sqrt{\omega/2}\,[\tau(\mathbf{r},\mathbf{x},\mathbf{r}_s)-\tau(\mathbf{r},\mathbf{x}_0,\mathbf{r}_s)]\}]. \tag{40}$$

The term under the integral over frequency has a damping term which prevents any arguments of equally balanced contributions for the whole frequency spectrum as it is for seismic inversion. This is a fundamental difference that we have underlined previously but we can argue that the main contribution to the integral is when the phase of the exponential is zero because the diffusive damping term is a slowly decaying function. If the background medium is sufficiently smooth, this occurs when $\mathbf{x}$ is close to $\mathbf{x}_0$. With local expansion of the pseudo-phase and the amplitude

$$\begin{aligned}\tau(\mathbf{r},\mathbf{x},\mathbf{r}_s) &\sim \tau(\mathbf{r},\mathbf{x}_0,\mathbf{r}_s) + \mathbf{p}\cdot(\mathbf{x}-\mathbf{x}_0)\\ A(\mathbf{r},\mathbf{x},\mathbf{r}_s) &\sim A(\mathbf{r},\mathbf{x}_0,\mathbf{r}_s)\end{aligned} \tag{41}$$

we find the asymptotic expression of the Hessian H

$$H(\mathbf{x},\mathbf{x}_0) \sim \frac{\mu_0^2}{4}\sum_{\mathbf{r}_s,\mathbf{r}}|\mathbf{p}(\mathbf{r},\mathbf{x}_0,\mathbf{r}_s)|^2 \times \int_0^\infty d\omega\sqrt{2\omega}\, e^{-\sqrt{2\omega}\tau(\mathbf{r},\mathbf{x}_0,\mathbf{r}_s)} e^{-\sqrt{\omega/2}\,\mathbf{p}\cdot(\mathbf{x}-\mathbf{x}_0)} \times \{\cos[\sqrt{\omega/2}\,\mathbf{p}\cdot(\mathbf{x}-\mathbf{x}_0)] - \sin\sqrt{\omega/2}\,\mathbf{p}\cdot(\mathbf{x}-\mathbf{x}_0)]\} \tag{42}$$

which has significant values when $\mathbf{x}$ is close to $\mathbf{x}_0$. We shall

The final and precise shape of the operator H is mainly controlled by the data acquisition geometry and eq. (44) should be considered only as an estimation for an iterative inversion method. The nearly diagonal structure of the operator H makes the computation of the inverse easier and leads to

$$\Delta\sigma(\mathbf{x}_0) = 1/H(\mathbf{x}_0, \mathbf{x}_0)\ \gamma_0(\mathbf{x}_0). \tag{45}$$

In order to check the final gradient expression (38) and the final Hessian expression (44), we have computed the reconstructed conductivity at a single diffracting point $\mathbf{x}_0$ from the scattered field computed by the Born approximation. We have deduced the exact conductivity contrast between the homogeneous reference medium and the scattering point. This analytical checking makes us confident in our expressions for imaging diffusive fields.

Iterative quasi-Newton inversion method

Let us note h the approximation of the Hessian H. The quasi-Newton solution of the inverse problem (29) is

$$\Delta\sigma(\mathbf{x})^{n+1} = \Delta\sigma(\mathbf{x})^n + h^{-1}\gamma^n \tag{46}$$

where γ^n is the gradient of the misfit function $S(\Delta\sigma)$ calculated around the value of $\Delta\sigma$ at the nth iteration:

$$\gamma^n = G^\dagger(\Delta E^{\text{obs}} - G\,\Delta\sigma^n). \tag{47}$$

As shown by Jin *et al.* (1992), the iterative method converges to the limit

$$\lim_{n\to\infty} \Delta\sigma^n = (\mathbf{G}^{-g}\mathbf{G})^{-1}\mathbf{G}^{-g}\,\Delta E^{\text{obs}} \tag{48}$$

which shows that the iterative method corrects for any bias in the Hessian estimation.

A self-consistent test

Before performing an inversion for a complete solution, we want to test the internal coherence of the linear inversion we propose. We have computed the Born approximation for a cylinder of radius 20 m at a depth of 100 m. The conductivity of the cylinder is $0.1\ \text{S m}^{-1}$ embedded in a homogeneous medium of conductivity $0.01\ \text{S m}^{-1}$. We consider a single line source right above the cylinder and five receivers at the free surface distributed by steps of 50 m on both sides of the source.

Figure 6 shows both the true cylinder and the recovered conductivity contrast. The recovered maximum value is only $0.01\ \text{S m}^{-1}$ while we should have found a value around $0.09\ \text{S m}^{-1}$. The wider extension of the recovered image explains this low maximum value. With the blurred image of Fig. 6, the predicted signals can explain most parts of the synthetic signals. Unfortunately, this is a drawback of the diffusion phenomenon which implies an integration over a pseudo-isochrone shell to recover the image. We find the typical 'smile' associated with the data acquisition geometry. During iterations, the misfit function decreases from 130 at the first iteration down to 66 at the 50th iteration.

If we consider other sources translated on the horizontal axis, we are able to stack different pictures of the medium and to improve our resolution. The cylinder shape is better resolved as expected in Fig. 7 with a noticeable reduction of the 'smile'. The misfit function goes down to 44 when normalized by the number of sources, lower than the misfit function for a single source. The extension of the recovered image still biases strongly the maximum amplitude of the conductivity contrast. We do expect better results when considering other geometries than the surface-to-surface geometry.

A test with the analytical complete solution

The previous test has been performed using Born computation as synthetic data. What happens when considering the exact solution of diffusion by a cylinder? We have already compared true and Born solutions in the frequency domain in a previous paragraph. From these analytical solutions in the frequency domain, we compute the solution in the time domain for the same geometry by fast Fourier transform. Then, we perform asymptotic inversions similar to the ones previously computed with Born synthetic solutions.

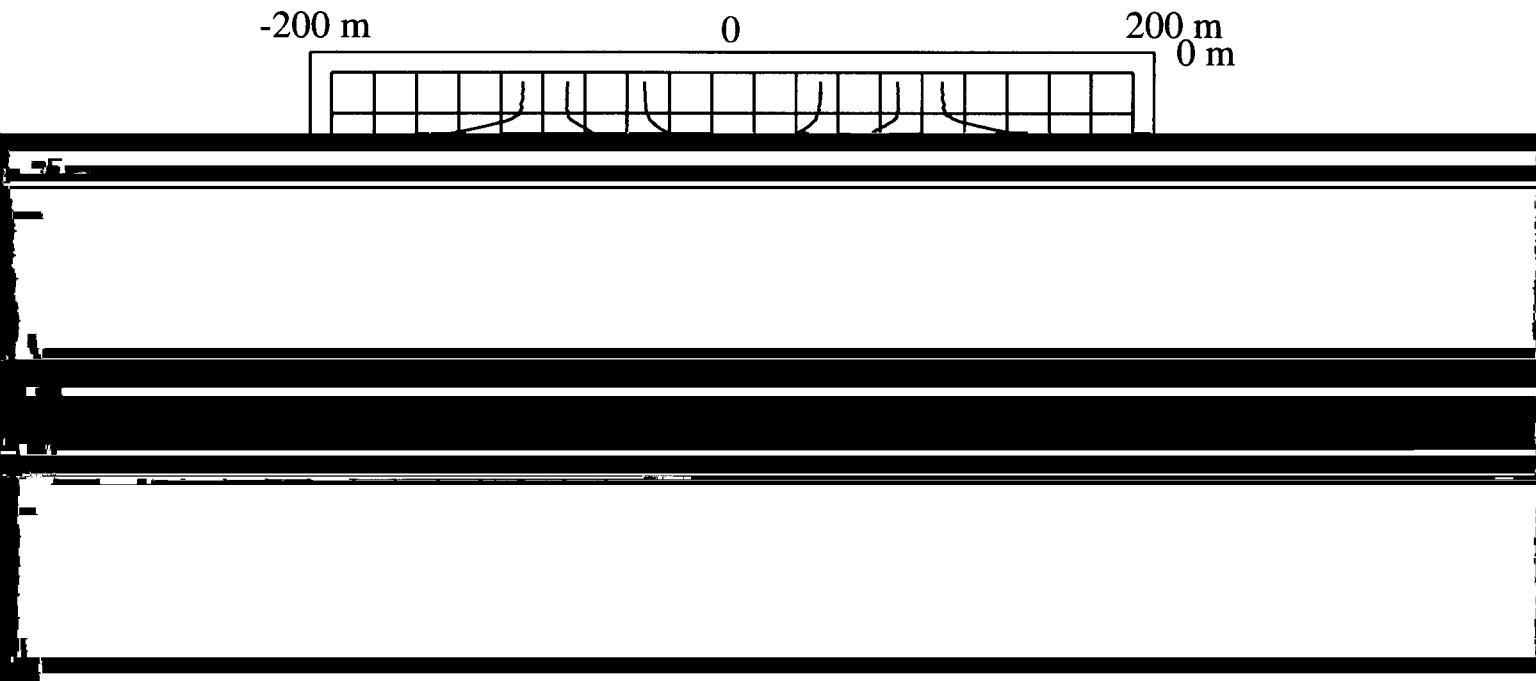

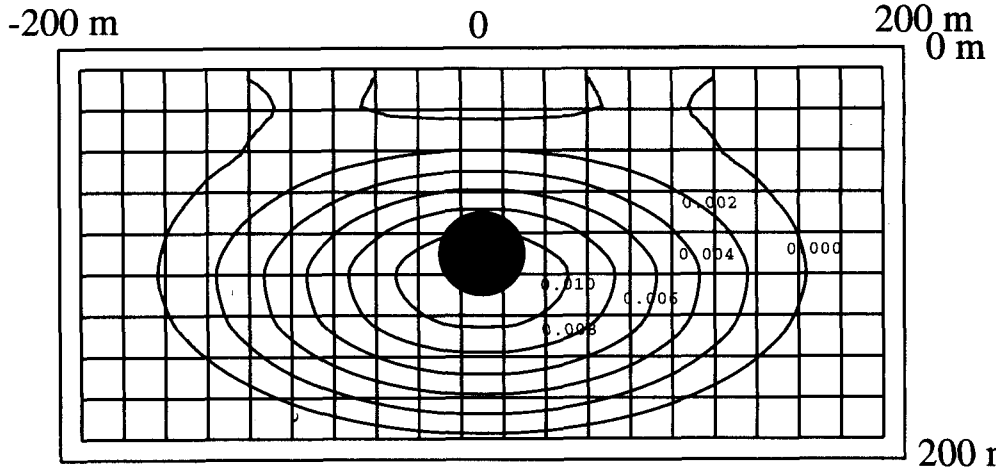

Figure 7. Conductivity contrast recovered after 50 iterations for five sources distributed at the free surface on both sides of the cylinder. Inverted data are the Born solution.

For inversion of the exact solution by a scattering cylinder, we find a deeper image with the typical 'smile' associated with one source geometry (see Fig. 8). The maximum amplitude of conductivity contrast is as high as 0.03 S m^{-1}. The amplitude difference between the Born solution and the complete solution in the time domain easily explains this amplification (see Fig. 9). The slight shift of the maximum diffusion pulse between these two solutions explains also why the image is deeper than the true cylinder. The reduction of the misfit function is from 475 at the first iteration to 166 at the 50th iteration. Fig. 9 gives an example of the residual signal left unexplained by the analytical inversion.

Performing the inversion using more sources removes the 'smile' geometry as shown in Fig. 10 but does not improve the position of the strongest conductivity amplitude which is still deeper than the true position. Changing the geometry structure by adding data recorded inside wells might improve this position problem already noticed with the Born approximation and amplified when using the exact solution.

We see in this final synthetic example the difficulty inherent in diffusion phenomena which blurs the image by the spatial extension of the so-called pseudo-isochrone shell for image recovering. This distortion of the image arises also from the Born approximation which, at intermediate frequencies, shows relatively poor agreement. Starting from a better reference medium with the already included low-frequency content of the conductivity might improve the picture, because, for the relatively higher spatial frequencies, the associated diffusion tail in time will be easier to handle.

DISCUSSION AND CONCLUSION

We have developed an analytical inversion for diffusive electromagnetism. This formalism draws its features from the seismic inversion approach. We extend the isochrone line concept of wave propagation to a pseudo-isochrone shell concept for diffusion. By doing so, we were able to construct an inversion scheme with explicit formula for the gradient and the Hessian of the misfit function. Because these formula are analytical, they are insensitive to noise

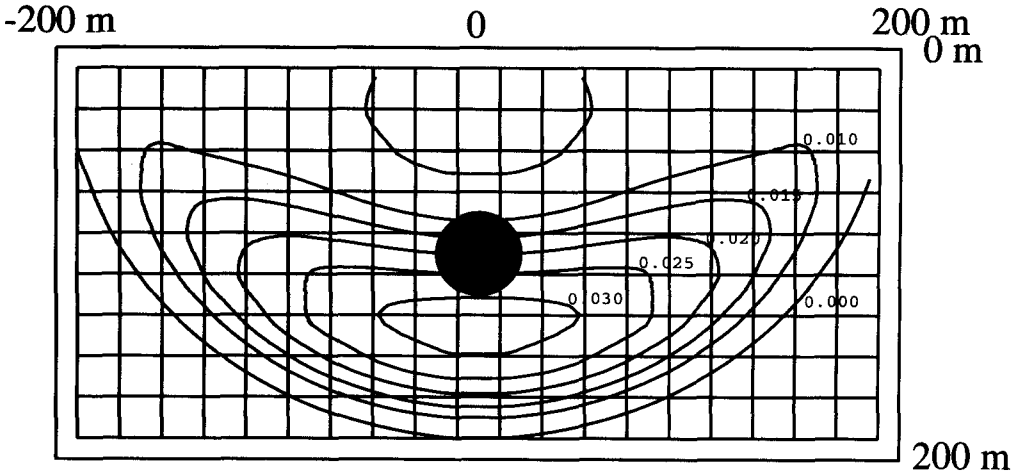

Figure 8. Conductivity contrast recovered after 50 iterations for one source at the free surface above the cylinder. Inverted solution is the exact analytical solution.

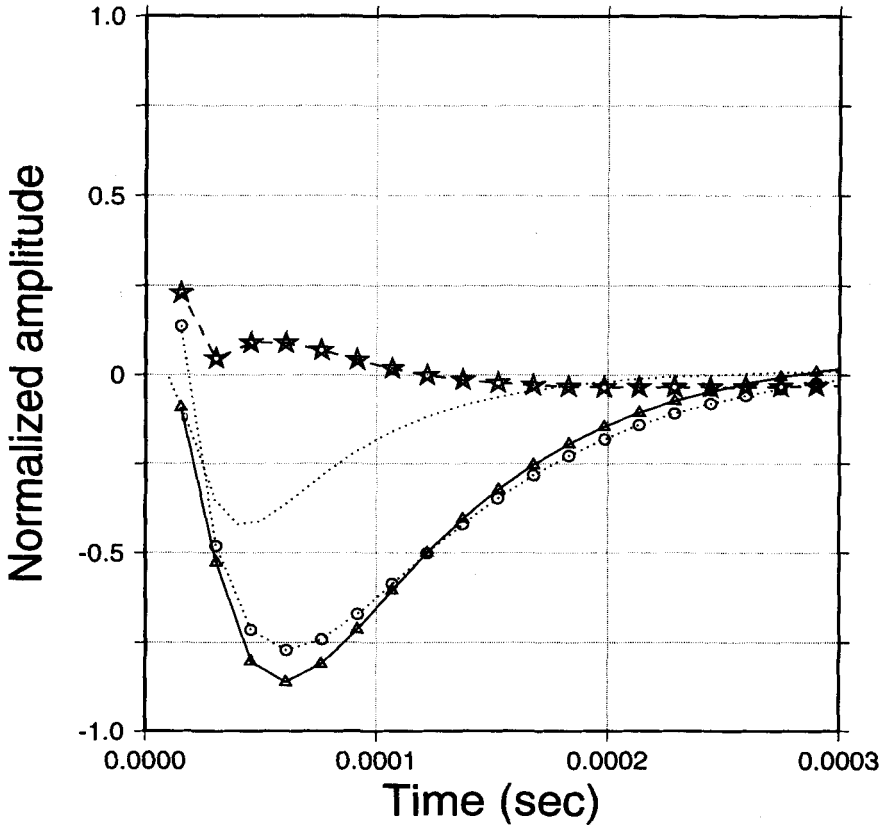

Figure 9. Synthetic electric signal (triangles) recorded at the receiver above the cylinder as well as the predicted signal (circles) computed for the cylinder image. The residual is also shown (diamonds), as well as the synthetic Born solution used in the forward modelling (dots).

which are simply not focused back into the medium when incoherent as already shown for seismic data (Lambaré *et al.* 1992).

The use of the Born approximation has limitations when we try to recover a spatially extended object on a homogeneous background. The possible extension to a smooth inhomogeneous reference medium will improve the position of heterogeneities by requiring only a fit of the relatively high-frequency part of the electric signal when the smooth background velocity has already been obtained. In that sense, this reconstruction technique is only a partial one in terms of spatial resolution.

In any case, we believe that, because the main diffusion pulse which is the one fitted in our present applications would have been already contained in our initial model, the spatially high-frequency content of the image will be better resolved. Of course, we might analyse the effect of noise for this inversion scheme as well as we might analyse performances on real data. This will be the purpose of object work.

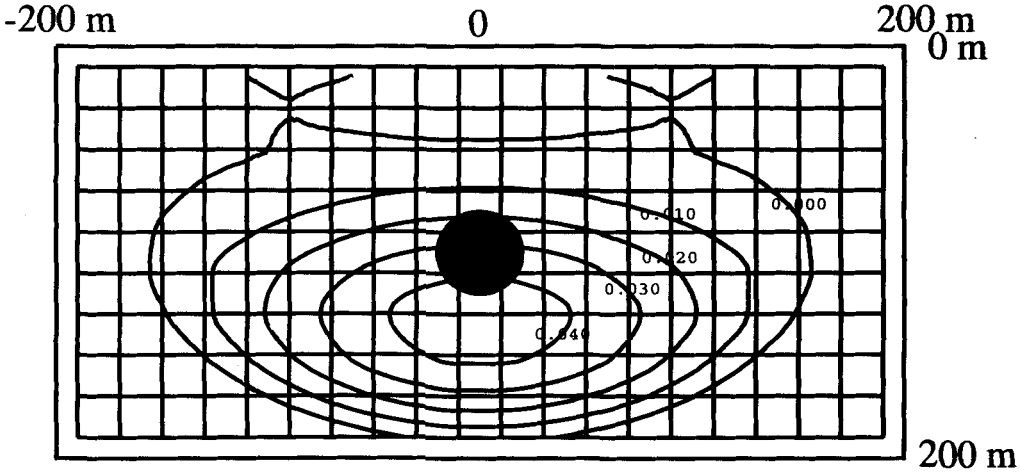

Figure 10. Conductivity contrast recovered after 50 iterations for five sources distributed at the free surface on both sides of the cylinder. The inverted solution is the exact analytical solution.

ACKNOWLEDGMENTS

This work was partly supported by the CNRS-INSU through the 'Tomographic' group and MEN-DRED through Jeune Equipe 'RuaDE'. We thank two anonymous reviewers for their helpful comments.

low-frequency electromagnetic fields, *Geophysics*, **58,** 780–796.

Lee, S., McMechan, G.A. & Aiken, C.L., 1987. Phase-field imaging: the electromagnetic equivalent of seismic migration, *Geophysics,* **52,** 1678–693.

Lee, K.H., Liu, G. & Morrison, H.F., 1989. A new approach to modeling the electromagnetic response of conductive media,